

Robust Fulde-Ferrell-Larkin-Ovchinnikov superfluidity in laser-assisted bilayer Fermi gases

Qing Sun,¹ Liang-Liang Wang,^{2,3} G. Juzeliūnas,^{4,*} and An-Chun Ji^{1,†}

¹*Department of Physics, Capital Normal University, Beijing 100048, China*

²*Institute for Natural Sciences, Westlake Institute for Advanced Study, Westlake University, Hangzhou, Zhejiang Province, China*

³*Westlake University, Hangzhou, Zhejiang Province, China*

⁴*Institute of Theoretical Physics and Astronomy, Vilnius University, A. Goštauto 12, Vilnius 01108, Lithuania*

(Dated: May 25, 2022)

Inspired by a recent observation of the supersolidity for bosonic atoms in a laser-assisted superlattice potential [J. Li, et. al., *Nature* 543, 91 (2017)], we consider an attractive two-component degenerate Fermi gas in a bilayer structure with two atomic hyperfine ground states involved. We find that the synthetic spin-orbit coupling (SOC) induced by the laser-assisted interlayer tunneling has a dramatical effect both on the two-body and many-body physics for atomic fermions. A bound molecular state appears, and the molecular dispersion can contain two minima at finite momenta even for vanishing intra- and inter-layer detunings. This is responsible for the pairing instability of the underlying attractive Fermi gas. As a result, the ground state of the system is found to be a Fulde-Ferrell-Larkin-Ovchinnikov (FFLO) superfluid with a spontaneous density-modulation of the order parameter. Due to the specific pairing mechanism in this system, the FFLO state is robust and appears in a wide parameter regime with the characteristic pairing momentum on the order of the SOC strength. The unique features of the two-body and many-body state can be observed in current experiments with ultracold atoms.

Since the prediction of the fermionic superfluidity with finite-momentum pairing [1, 2], the Fulde-Ferrell-Larkin-Ovchinnikov (FFLO) state has been studied for many decades in various systems ranging from the condensed matter physics to nuclear physics [3–5]. Among them, the ultracold atoms with a high tunability of the parameters represent a new and unique platform to investigate this exotic state. Despite numerous attempts to observe the FFLO state in various systems [6–8], its existence remains elusive. A realization of the one-dimensional (1D) spin-orbit coupling (SOC) for ultracold atoms [9–14] provides new insights to achieve the FFLO superfluidity [15–23]. Due to the absence of Galilean invariance in these systems, the bound dimers may carry finite center-of-mass (COM) momenta for nonvanishing Zeeman fields, and the system can exhibit the FFLO state at low temperature. However the Raman coupling inducing such a 1D SOC [9–13] involves the spin-flip transitions accompanied by heating, and a more sophisticated 2D SOC [24] invoked in many proposals [25–34] suffers even larger losses [32, 33] preventing from observing the FFLO states in current experiments.

Recently an effective one-dimensional (1D) SOC has been implemented for bosonic atoms using laser-assisted tunneling between the sites of a double well potential, the atomic states localized in each well representing the (quasi-)spin states [14, 35, 36]. The scheme does not require the Raman induced spin flip transitions, so the heating can be strongly suppressed. Using such a scheme supersolid properties associated with the Bose-Einstein condensation in two momentum states have been observed [35]. This sheds light on the realization of FFLO

state for the fermions in such a system, since the FFLO state has supersolid properties [37].

Here we demonstrate a possibility of formation of the FFLO state for a two-component Fermi gas with attractive interactions in a bilayer system. In that case the atomic states localized in different layers play a role of the quasi-spin states, and the laser assisted interlayer tunneling provides effectively the 1D SOC between the layer states without the lossy spin-flip transitions involved. An interplay between the effective interlayer spin-orbit coupling and the interaction between atoms in different internal states in the same layer gives rise to bound dimer states characterized by two minima at finite COM momenta. This is responsible for the pairing instability of the underlying attractive Fermi gas. In fact, the many-body ground state is found to be a FFLO superfluid, carrying finite momenta even for vanishing Zeeman fields. Since the atoms with opposite momenta are located mainly in different layers and the atomic attraction dominates in the same layer, the FFLO state is robust in a wide parameter range.

The Model. – We consider a two-component Fermi gas composed of atoms in two metastable internal (quasi-spin) states labeled by the index $\gamma = \uparrow, \downarrow$. These could be for example two hyperfine atomic ground states. The atoms are confined in a state-independent double-well optical potential along the z -axis providing a bilayer structure [14]. An asymmetry of the double well potential prevents a direct atomic tunneling between the wells, and instead there is a laser-assisted interlayer tunneling. The second-quantized Hamiltonian for atoms in such a bilayer

system reads in the momentum representation

$$\mathcal{H} = \sum_{\mathbf{k}\gamma} \left[\sum_j \xi_{\mathbf{k}\gamma j} \hat{\psi}_{\mathbf{k}\gamma j}^\dagger \hat{\psi}_{\mathbf{k}\gamma j} + \frac{\mathcal{J}}{2} (\hat{\psi}_{\mathbf{k}\gamma,1}^\dagger \hat{\psi}_{\mathbf{k}\gamma,2} + h.c.) \right] + \frac{U}{S} \sum_{\mathbf{k}\mathbf{k}'\mathbf{q}j} \hat{\psi}_{\mathbf{k}\uparrow j}^\dagger \hat{\psi}_{\mathbf{k}'\downarrow j}^\dagger \hat{\psi}_{\mathbf{k}'+\mathbf{q}\downarrow j} \hat{\psi}_{\mathbf{k}-\mathbf{q}\uparrow j}, \quad (1)$$

with

$$\xi_{\mathbf{k}\gamma j} = \frac{1}{2} [(\mathbf{k} + (-1)^{j+1} \kappa \mathbf{e}_x)^2 + h(-1)^j \pm \delta], \quad (2)$$

where the upper and lower signs in Eq. (2) correspond to different atomic components $\gamma = \uparrow, \downarrow$, and the atomic mass m and \hbar are set to the unity. Here also $\hat{\psi}_{\mathbf{k}\gamma j}^\dagger$ and $\hat{\psi}_{\mathbf{k}\gamma j}$ are Fermi operators for creation and annihilation of an atom in the j th layer ($j = 1, 2$) with an internal state γ and a momentum \mathbf{k} in the xy (layer) plane; h and δ denote the energy mismatch between the two layers and two components, respectively; \mathcal{J} is a strength of the laser-assisted interlayer tunneling with $2\kappa\mathbf{e}_x$ being an associated recoil momentum shift along the x -direction. The latter recoil is represented by the layer-dependent momentum shift $(-1)^{j+1} \kappa \mathbf{e}_x$ in Eq. (2). This provides a 1D (along the x -direction) SOC between the layer states, the SOC being the same for both atomic internal states.

In Eq.(1) the atom-atom coupling is represented by the contact interaction between the atoms within individual layers and in different internal states $\gamma = \uparrow, \downarrow$ [38]. This provides the singlet intralayer interaction. The bare contact interaction U should be renormalized as $\frac{1}{U} = -\frac{1}{S} \sum_{\mathbf{k}} \frac{1}{E_b + 2\epsilon_{\mathbf{k}}}$ [39] in the Hamiltonian (1), where E_b is a binding energy of the two-body bound state in the absence of SOC, S is a two-dimensional (2D) quantization volume and $\epsilon_{\mathbf{k}} = \mathbf{k}^2/2$ is a 2D free particle dispersion. For ultracold atoms E_b can be tuned via the Feshbach resonance technique [40].

Two-body Problem. – Let us first give some remarks on the single-particle problem. In this paper, we shall concentrate on the most interesting case of zero detuning between the layers and the components, $h = \delta = 0$; the situation where $h, \delta \neq 0$ will be discussed later. In the absence of the atom-atom interaction, both components have the same single particle spectra characterized by two dispersion branches $\epsilon_{\mathbf{k}\pm} = \frac{\mathbf{k}^2 + \kappa^2}{2} \pm \sqrt{k_x^2 \kappa^2 + \frac{\mathcal{J}^2}{4}}$. The minimum of the lower branch $\epsilon_{\mathbf{k}-}$ gives the energy of the single-particle ground state. For $\mathcal{J} < \mathcal{J}_c$ the ground state energy has two minima with momenta $k_x = \pm \sqrt{\frac{4\kappa^4 - \mathcal{J}^2}{4\kappa^2}}$, where $\mathcal{J}_c = 2\kappa^2 = 4E_\kappa$ is the critical interlayer tunneling strength, $E_\kappa = \kappa^2/2$ being the recoil energy. The two minima merge to a single minimum at $k_x = 0$ for $\mathcal{J} \geq \mathcal{J}_c$.

The attraction between atoms can lead to formation of the bound molecular states which are constructed as

$$|\Phi\rangle_{\mathbf{q}} = \frac{1}{2} \sum_{\mathbf{k}} \sum_{j,l=1}^2 \phi_{\mathbf{k}\mathbf{q},jl} S_{\mathbf{k}\mathbf{q},jl}^\dagger |0\rangle, \quad (3)$$

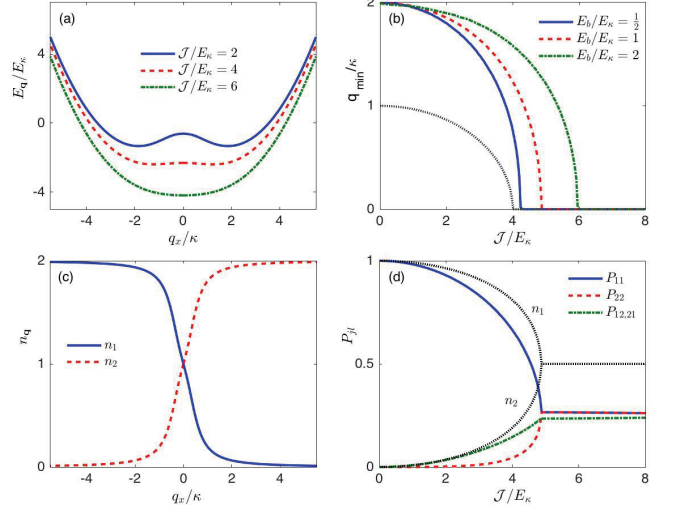


FIG. 1: Color online. (a) The molecular energy $E_{\mathbf{q}}$ as a function of COM momentum $\mathbf{q} = q_x \hat{\mathbf{e}}_x$ at $E_b/E_\kappa = 1$, for $\mathcal{J}/E_\kappa = 2$ (blue solid), 4 (red dashed), and 6 (green dash-dotted). (b) The momentum of the ground-state molecular as a function of the tunneling strength \mathcal{J} for atomic interaction $E_b/E_\kappa = 0.5$ (blue solid), 1 (red dashed), and 2 (green dash-dotted). As a comparison, the single-particle ground-state momentum is also given (black dotted). (c) The atomic density distribution $n_{\mathbf{q}}$ in each layer as a function of COM momentum $\mathbf{q} = q_x \hat{\mathbf{e}}_x$ for $\mathcal{J}/E_\kappa = 2$ and $E_b/E_\kappa = 1$. (d) Evolution of the singlet population P_{jl} and the intralayer atomic density $n_{1,2}$ for one of the degenerate ground molecular with $\mathbf{q}_0 = -q_{\min} \mathbf{e}_x$ at $E_b/E_\kappa = 1$. The energy and momentum are measured in units of $E_\kappa = \kappa^2/2$ and κ , respectively.

with

$$S_{\mathbf{k}\mathbf{q},jl}^\dagger = \frac{1}{\sqrt{2}} [\psi_{j\uparrow}^\dagger(\mathbf{Q}_+) \psi_{l\downarrow}^\dagger(\mathbf{Q}_-) - \psi_{j\downarrow}^\dagger(\mathbf{Q}_+) \psi_{l\uparrow}^\dagger(\mathbf{Q}_-)] \quad (4)$$

and $\mathbf{Q}_\pm = \mathbf{q}/2 \pm \mathbf{k}$. Here $S_{\mathbf{k}\mathbf{q},jl}^\dagger$ is a singlet operator for creating a pair of atoms in the layers j and l with a COM momentum \mathbf{q} and a relative momentum \mathbf{k} , and $\phi_{\mathbf{k}\mathbf{q},jl}$ is the corresponding amplitude. For $j = l$ the atoms are paired in the same layer, whereas for $j \neq l$ the pairing takes place in different layers, the latter contribution emerging due to the laser-assisted tunneling. Since $S_{-\mathbf{k}\mathbf{q},jl}^\dagger = S_{\mathbf{k}\mathbf{q},lj}^\dagger$, we take $\phi_{-\mathbf{k}\mathbf{q},jl} = \phi_{\mathbf{k}\mathbf{q},lj}$ in Eq. (3), in which the factor 1/2 is to avoid a double counting of the atomic states. The molecular state does not contain the triplet contributions, because the spin-independent laser assisted interlayer tunneling featured in the Hamiltonian (1) preserves the singlet state.

Substituting Eq.(3) into the stationary Schrödinger equation $\mathcal{H}|\Phi\rangle_{\mathbf{q}} = E_{\mathbf{q}}|\Phi\rangle_{\mathbf{q}}$, one arrives at the following equation for the molecular energy $E_{\mathbf{q}}$ (see SM for details).

$$\left(\frac{U}{S} \sum_{\mathbf{k}} \frac{\alpha_{\mathbf{k}}}{\alpha_{\mathbf{k}} \gamma_{\mathbf{k}} - \beta_{\mathbf{k}}^2} - 1 \right) \left(\frac{U}{S} \sum_{\mathbf{k}} \frac{\gamma_{\mathbf{k}}}{\alpha_{\mathbf{k}} \gamma_{\mathbf{k}} - \beta_{\mathbf{k}}^2} - 1 \right) - \left(\frac{U}{S} \sum_{\mathbf{k}} \frac{\beta_{\mathbf{k}}}{\alpha_{\mathbf{k}} \gamma_{\mathbf{k}} - \beta_{\mathbf{k}}^2} \right)^2 = 0, \quad (5)$$

where $\alpha_{\mathbf{k}} = E_{\mathbf{q}} - (\mathbf{k}^2 + \mathbf{q}^2/4 + \kappa^2)$, $\beta_{\mathbf{k}} = q_x \kappa$ and $\gamma_{\mathbf{k}} = \alpha_{\mathbf{k}} - \{\frac{\mathcal{J}^2/2}{\alpha_{\mathbf{k}}+2k_x\kappa} + \frac{\mathcal{J}^2/2}{\alpha_{\mathbf{k}}-2k_x\kappa}\}$. For a vanishing recoil of the interlayer tunneling, $\kappa = 0$, one arrives at two bound-state branches with binding energies $E_b^{(1)} = \sqrt{E_b^2 + \mathcal{J}^2} - \mathcal{J}$ and $E_b^{(2)} = E_b - \mathcal{J}$, and the ground state always occurs at $\mathbf{q} = 0$. On the other hand, for $\kappa \neq 0$, these two branches get mixed, and a finite COM momentum $\mathbf{q} \neq 0$ may develop for the two-body ground state. By numerically solving Eq. (5) we find the energy of the two-body bound state $E_{\mathbf{q}}$ as a function of the COM momentum \mathbf{q} . Like the single-particle dispersion, the energy spectrum $E_{\mathbf{q}}$ can contain two degenerate minima at $\mathbf{q}_0 = \pm q_{\min} \mathbf{e}_x$ for certain values of \mathcal{J} and E_b , as shown in Fig. 1a. Such a unique property of the bilayer system is in a sharp contrast with the SOC for real spins, where the bound state always minimizes at $\mathbf{q} = 0$ for zero interspin detuning ($\delta = 0$) [22]. Moreover, at the single-particle critical point $\mathcal{J}_c/E_{\kappa} = 4$, the molecular state is still formed at nonzero momentum (see the red dashed line in Fig. 1a). This suggests that the atomic interaction plays an essential role to induce the pairing with finite COM momentum in the bilayer system.

Figure 1b illustrates the evolution of the minimum momentum $q_{\min} = |\mathbf{q}_0|$ with the tunneling strength \mathcal{J} for the fixed atomic interaction energy E_b . If \mathcal{J}/E_{κ} is smaller than the unity, one has $q_{\min} \sim 2\kappa$. Subsequently q_{\min} decreases continuously with \mathcal{J} , and eventually becomes zero when \mathcal{J} exceeds the critical value. Furthermore, the critical tunneling is found to increase with the atomic interaction E_b , suggesting that a stronger attraction between atoms would be more favorable for forming the finite-momentum molecular state.

To understand the underlying physics, in Fig. 1c we plot a typical density distribution $n_j = \sum_{\gamma} n_{j\gamma}$ of the molecular state as a function of the COM momentum \mathbf{q} . Here $n_{j\gamma} = \sum_{\mathbf{k}} \langle \psi_{\mathbf{k}\gamma j}^{\dagger} \psi_{\mathbf{k}\gamma j} \rangle_{\mathbf{q}}$ is a density of atoms in the j th layer and the internal state γ , with $\langle \dots \rangle_{\mathbf{q}}$ denoting an expectation value for the molecular state $|\Phi\rangle_{\mathbf{q}}$. Notice that we have $n_{j\uparrow} = n_{j\downarrow}$ and $n_1(\mathbf{q}) = n_2(-\mathbf{q})$. Due to the interlayer SOC, the molecules with negative (positive) COM momentum are mainly formed by the atoms in the first (second) layer, and only close to the zero momentum both layers have comparable contributions. To be specific, in Fig. 1d, we plot the population of the four singlet spin-layer states $P_{jl} = \sum_{\mathbf{k}} |\phi_{\mathbf{kq},jl}|^2$ and the corresponding relative atomic populations $n_{1,2}$ in two layers as a function of the tunneling strength \mathcal{J} for a ground molecular state forming at $\mathbf{q}_0 = -q_{\min} \mathbf{e}_x$. For $\mathcal{J}/E_{\kappa} < 1$, the intralayer singlet pairing in the first layer is dominant (the blue line in Fig. 1d). Since both spin components in the first layer have the same tunneling-induced momentum shift $-\kappa \mathbf{e}_x$ [in the layer-dependent frame used in Eqs. (1)-(2)], the bound dimer located in the first layer tends to carry the momentum $\mathbf{q}_0 = -q_{\min} \mathbf{e}_x$ with $q_{\min} \sim 2\kappa$. As the tunneling strength

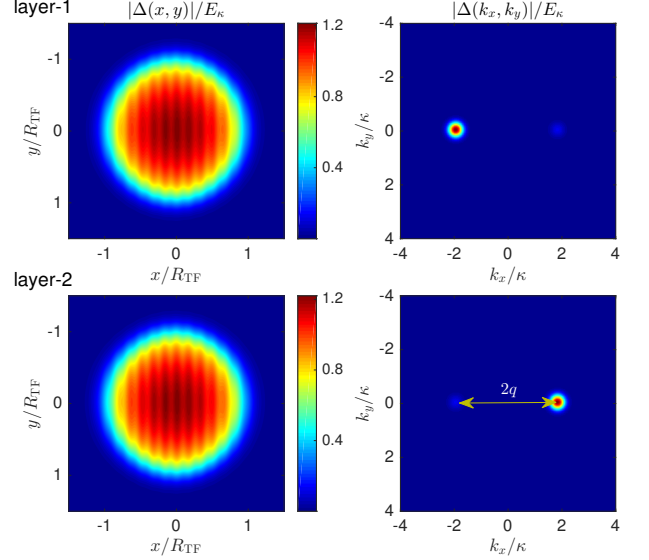


FIG. 2: Color online. Real-space density profile (left panel) and momentum space distribution (right panel) of the superfluid order parameters $\Delta_{1,2}$ for $\mathcal{J}/E_{\kappa} = 2$. In the simulations, we have also included a weak harmonic trap with frequency $\omega \ll E_{\kappa}$. Here, $2q = |\mathbf{q}_1 - \mathbf{q}_2|$, $R_{\text{TF}} \equiv \sqrt{2E_{\kappa}/m\omega^2} = \kappa/\omega$ and $E_b/E_{\kappa} = 1$.

is increased, the atoms in two layers get mixed, and the interlayer singlet components become significant. Thus there is a considerable contribution from the atoms in the second layer with the opposite momentum shift $\kappa \mathbf{e}_x$, giving rise to a decrease in the molecular COM momentum q_{\min} . For $\mathcal{J}/E_{\kappa} \gg 1$, both layers have equal atomic populations with equal weight intralayer singlet components, the opposite momenta are compensated in each layer resulting in a zero momentum molecular state.

The FFLO superfluidity. – The two-body results obtained above would have dramatic effects when we consider a gas of fermions. As we will see in the following, the many-body ground state in this system is a superfluid with the density modulation, i.e. the FFLO state. Intuitively from the single-particle spectrum containing two minima due to the interlayer SOC, the atoms with opposite momenta are mainly situated at different layers for different components. On the other hand, the attractive interactions between different atomic internal states takes place in the same layer [38]. As a result, at the Fermi surface, the zero-momentum pairing between the two components would be largely suppressed and the ground state may carry a nonvanishing momentum.

To verify this assumption, we have numerically solved the Bogoliubov-de Gennes (BdG) equation of the system for finding the ground state. To this end, we introduce the superfluid order parameters $\Delta_j(\mathbf{r}) = -U \langle \hat{\psi}_{j,\downarrow}(\mathbf{r}) \hat{\psi}_{j,\uparrow}(\mathbf{r}) \rangle$ for the layers $j = 1, 2$, with $\mathbf{r} = (x, y)$, and write down the BdG equation as $H_{\text{BdG}}(\mathbf{r})\phi_{\eta} = \varepsilon_{\eta}\phi_{\eta}$, with H_{BdG} being a

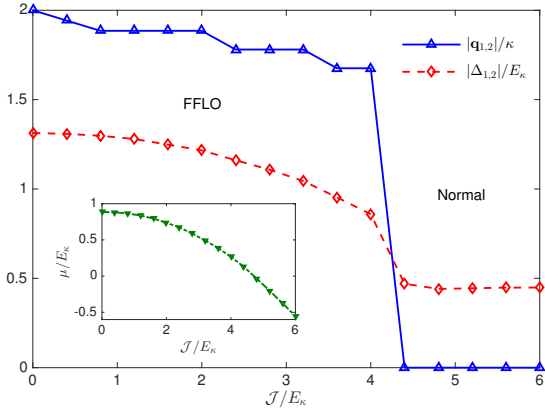


FIG. 3: Color online. The order parameter $\Delta_{1,2}$ (maximum of the order parameter in the whole region) (red solid) and the magnitude of the FFLO vector $|\mathbf{q}_{1,2}|$ (blue dashed) as functions of the tunneling strength J/E_κ . The inset shows the evolution of the chemical potential μ . $E_b/E_\kappa = 1$.

8×8 matrix (see SM for the explicit form). Here $\phi_\eta = [u_{1\uparrow,\eta}, u_{1\downarrow,\eta}, v_{1\uparrow,\eta}, v_{1\downarrow,\eta}, u_{2\uparrow,\eta}, u_{2\downarrow,\eta}, v_{2\uparrow,\eta}, v_{2\downarrow,\eta}]^T$ is the Nambu basis and ε_η is the corresponding energy of Bogoliubov quasiparticles labeled by an index η . In this basis, the order parameters $\Delta_j(\mathbf{r})$ for each layer become

$$\Delta_j(\mathbf{r}) = -U \sum_\eta [u_{j\uparrow,\eta} v_{j\downarrow,\eta}^* f(-\varepsilon_\eta) + u_{j\downarrow,\eta} v_{j\uparrow,\eta}^* f(\varepsilon_\eta)], \quad (6)$$

where $f(E) = 1/(e^{E/k_B T} + 1)$ is the Fermi-Dirac distribution function at a temperature T . In this paper, we mainly consider the zero temperature case. The atom number is given by $N = \int d\mathbf{r} n(\mathbf{r})$, with

$$n(\mathbf{r}) = \sum_{j\sigma,\eta} [|u_{j\sigma,\eta}(\mathbf{r})|^2 f(\varepsilon_\eta) + |v_{j\sigma,\eta}(\mathbf{r})|^2 f(-\varepsilon_\eta)]. \quad (7)$$

being the atomic density [41].

Self-consistently solving Eqs. (6) and (7) with the basis expansion method [42], one can readily obtain the ground state configuration of the system. In Fig. 2, we present the order parameter configuration at a moderate tunneling $J/E_\kappa = 2$ for a fixed interaction strength $E_b/E_\kappa = 1$. Significantly, one can observe that the system is in a superfluid phase with the order parameter $\Delta_{1,2}$ exhibiting a density modulation in the real-space profile (left panel of Fig. 2). The density stripes are seen even clearer in the momentum distribution of $\Delta_{1,2}$, where two peaks at opposite momenta $\mathbf{q}_{1,2} \sim \pm 1.9\kappa\mathbf{e}_x$ (right panel of Fig. 2) can be identified. This suggests that the atomic pairing occurs at finite momenta, a key property of the FFLO state.

The unique features of the paring wave function $\Delta_{1,2}$ are consistent with the results of the two-body problem, which can be viewed qualitatively as a superposition of the bound molecular states at the double minima with opposite momenta. Furthermore for tunneling strength

J smaller than the recoil energy E_κ , the interlayer SOC induces a large imbalance of the momentum distribution between the two layers for both spin states (see Fig. 1c). As a result, the amplitudes at two opposite pairing momenta become asymmetric, with one of the two pairing components being much larger than the other in each layer, as shown in the right panel of Fig. 2. Such a pairing imbalance in two layers decreases with the strength of the tunneling which tends to mix the momentum states in different layers, giving rise to a more prominent density profile in the order parameter.

Figure 3 illustrates the evolution of the order parameter $|\Delta_{1,2}|$ and the pairing momentum $|\mathbf{q}_{1,2}|$ as functions of the tunneling strength J . One can observe that with the increase of J , the COM momentum $|\mathbf{q}_{1,2}|$ decreases gradually and eventually vanishes at a critical value of the tunneling strength. This defines a transition from the FFLO state to the normal superfluid with zero momentum. Across the transition, the chemical potential μ decreases continuously (see the inset in Fig. 3).

So far we have discussed the situation where $h = \delta = 0$, so the populations of both spin and layer states are balanced. For a non-zero detuning between the spin energies ($\delta \neq 0$), the spin populations become imbalanced with mismatched Fermi surfaces, leading to the FFLO states [1, 2]. However, the parameter region of the FFLO states is quite narrow in the absence of SOC [43–46]. As the two-body molecular spectrum of the system is not affected by δ (see SM for detail), this would leave the main physics discussed above unchanged. For a non-zero interlayer detuning ($h \neq 0$), the degeneracy of the double minima in the single-particle and two-body bound state spectra are lifted, with an imbalanced layer population of atoms. As in our system h plays a role of the Zeeman field, it is more beneficial to achieve the FFLO state for $h \neq 0$, which has been also confirmed by the numerical simulations.

Finally, we discuss some experiment-related issues. The laser-assisted SOC in the bilayer system can be applied both for the Bose- and Fermi- atoms. In current experiments, the bilayer geometry can be implemented using the double-well superlattice potential, which would form a stack of weakly coupled bilayer systems increasing the signal-to-noise ratio. In the bilayer system the typical pairing momentum \mathbf{q} of the FFLO state is on the order of κ for a moderate tunneling strength J . This gives rise to a periodicity $\pi/|\mathbf{q}| \sim \pi/\kappa$ of the stripes, which can be readily detected by the optical Brag scattering [35].

In conclusion, we have considered the two-component degenerate Fermi gas in the bilayer system, in which the atomic states localized in different layers play a role of the quasi-spin states. The laser assisted interlayer tunneling provides effectively the 1D SOC between the layer states, without involving lossy spin-flip transitions. Such a synthetic SOC plays a fundamental role for attractive Fermi gases. A bound molecular state is found, with

a dispersion containing two minima at finite momenta. This leads to the pairing instability of the underlying attractive Fermi gas at finite momenta, and a robust FFLO superfluidity appears accompanied by a spontaneous density-modulation of the order parameter, with a characteristic pairing momentum being on the order of the SOC strength. The unique features of the FFLO state and the two-body bound state in this system can be observed for ultracold atoms with current experimental techniques.

This work is supported by the NSFC under Grants No. 11404225, No. 11474205, and No.11504037. G.J. acknowledges support by the Lithuanian Research Council (Grant No. MIP- 086/2015).

* Electronic address: gediminas.juzeliunas@tfai.vu.lt

† Electronic address: andrewjee@sina.com

- [1] P. Fulde and R. A. Ferrell, Phys. Rev. **135**, A550 (1964).
- [2] A. I. Larkin and Y. N. Ovchinnikov, Zh. Eksp. Teor. Fiz. **47**, 1136 (1964).
- [3] K. B. Gubbels and H. T. C. Stoof, Phys. Rep. **525**, 255 (2012).
- [4] R. Casalbuoni and G. Nardulli, Rev. Mod. Phys. **76**, 263 (2004).
- [5] R. Anglani, R. Casalbuoni, M. Ciminale, R. Gatto, N. Ippolito, M. Mannarelli, and M. Ruggieri, Rev. Mod. Phys. **86**, 509 (2014).
- [6] T. Mizushima, K. Machida, and M. Ichioka, Phys. Rev. Lett. **94**, 060404 (2005).
- [7] Y.-A. Liao, A. Rittner, T. Paprotta, W. Li, G. Partridge, R. Hulet, S. Baur, and E. Mueller, Nature **467**, 567 (2010).
- [8] L. Radzihovsky and D. E Sheehy, Rep. Prog. Phys. **73**, 076501 (2010).
- [9] Y.-J. Lin, K. Jiménez-García, and I. B. Spielman, Nature (London) **471**, 83 (2011).
- [10] J.-Y. Zhang, S.-C. Ji, Z. Chen, L. Zhang, Z.-D. Du, B. Yan, G.-S. Pan, B. Zhao, Y.-J. Deng, H. Zhai, S. Chen, and J.-W. Pan, Phys. Rev. Lett. **109**, 115301 (2012).
- [11] P. J. Wang, Z.-Q. Yu, Z. K. Fu, J. Miao, L. H. Huang, S. J. Chai, H. Zhai, and J. Zhang, Phys. Rev. Lett. **109**, 095301 (2012).
- [12] L. W. Cheuk, A. T. Sommer, Z. Hadzibabic, T. Yefsah, W. S. Bakr, and M. W. Zwierlein, Phys. Rev. Lett. **109**, 095302 (2012).
- [13] C. Qu, C. Hamner, M. Gong, C. W. Zhang, P. Engels, Phys. Rev. A **88**, 021604(R) (2013).
- [14] J. Li, W. Huang, B. Shteynas, S. Burchesky, F. C. Top, E. Su, J. Lee, A. O. Jamison, and W. Ketterle, Phys. Rev. Lett. **117**, 185301 (2016).
- [15] C. Chen, Phys. Rev. Lett. **111**, 235302 (2013).
- [16] M. Iskin and A. L. Subasi, Phys. Rev. A **87**, 063627 (2013).
- [17] V. B. Shenoy, Phys. Rev. A 88, 033609 (2013).
- [18] X.-J. Liu and H. Hu, Phys. Rev. A **88**, 023622 (2013).
- [19] F. Wu, G. C. Guo, W. Zhang, and W. Yi, Phys. Rev. Lett. **110**, 110401 (2013).
- [20] C. Qu, Z. Zheng, M. Gong, Y. Xu, L. Mao, X. Zou, G. Guo, and C. Zhang, Nat. Commun. **4**, 2710 (2013).
- [21] W. Zhang and W. Yi, Nat. Commun. **4**, 2711 (2013).
- [22] L. Dong, L. Jiang, H. Hu, and H. Pu, Phys. Rev. A **87**, 043616 (2013); L. Dong, L. Jiang, and H. Pu, New J. Phys. **15** 075014 (2013).
- [23] Z. Zheng, M. Gong, X. Zou, C. Zhang, and G. G. Guo, Phys. Rev. A **87**, 031602(R) (2013); Z. Zheng, C. Qu, X. Zou, and C. Zhang, Phys. Rev. Lett. **116**, 120403 (2016).
- [24] N. Goldman, G. Juzeliūnas, P. Öhberg, and I. B. Spielman, Rep. Prog. Phys. **77**, 126401 (2014).
- [25] J. Ruseckas, G. Juzeliūnas, P. Öhberg, and M. Fleischhauer, Phys. Rev. Lett. **95**, 010404 (2005).
- [26] G. Juzeliūnas, J. Ruseckas, and J. Dalibard, Phys. Rev. A **81**, 053403 (2010).
- [27] C. Zhang, Phys. Rev. A **82**, 021607(R) (2010).
- [28] D. L. Campbell, G. Juzeliūnas, and I. B. Spielman, Phys. Rev. A **84**, 025602 (2011).
- [29] X.-J. Liu, K. T. Law, and T. K. Ng, Phys. Rev. Lett. **112**, 086401 (2014).
- [30] Q. Sun, L. Wen, W.-M. Liu, G. Juzeliūnas, and A.-C. Ji, Phys. Rev. A **91**, 033619 (2015).
- [31] S.-W. Su, S.-C. Gou, Q. Sun, L. Wen, W.-M. Liu, A.-C. Ji, J. Ruseckas, and G. Juzeliūnas, Phys. Rev. A **93**, 053630 (2016).
- [32] L. Huang, Z. Meng, P. Wang, P. Peng, S.-L. Zhang, L. Chen, D. Li, Q. Zhou, and J. Zhang, Nat. Phys. **12**, 540 (2016).
- [33] Z. Meng, L. Huang, P. Peng, D. Li, L. Chen, Y. Xu, C. Zhang, P. Wang, and J. Zhang, Phys. Rev. Lett. **117**, 235304 (2016).
- [34] Z. Wu, L. Zhang, W. Sun, X.-T. Xu, B.-Z. Wang, S.-C. Ji, Y. Deng, S. Chen, X.-J. Liu, and J.-W. Pan Science **354**, 83 (2016).
- [35] J. Li, J. Lee, W. Huang, S. Burchesky, B. Shteynas, F. C. Top, A. O. Jamison, and W. Ketterle, Nature **543**, 91 (2017).
- [36] Q. Sun, J. Hu, L. Wen, W.-M. Liu, G. Juzeliūnas, and An-Chun Ji, Sci. Rep. **6**, 37679 (2016).
- [37] A. Bulgac and M. M. Forbes, Phys. Rev. Lett. **101**, 215301 (2008).
- [38] The interlayer atomic interaction is neglected due to the overlap of the wave-function for atoms in different layer is exponentially smaller than that in the same layer [14].
- [39] M. Randeria, J.-M. Duan, and L.-Y. Shieh, Phys. Rev. Lett. **62**, 981 (1989).
- [40] C. Chin, R. Grimm, P. Julienne, and E. Tiesinga, Rev. Mod. Phys. **82**, 1225 (2010).
- [41] For $\delta = 0$, we always have $N_\uparrow = N_\downarrow$.
- [42] Y. Xu, L. Mao, B. Wu, and C. Zhang, Phys. Rev. Lett. **113**, 130404 (2014).
- [43] M. W. Zwierlein, A. Schirotzek, C. H. Schunck, and W. Ketterle, Science **311**, 492 (2006).
- [44] G. B. Partridge, W. Li, R. I. Kamar, Y. Liao, and R. G. Hulet, Science **311**, 503 (2006).
- [45] D. E. Sheehy and L. Radzihovsky, Phys. Rev. Lett. **96**, 060401 (2006).
- [46] H. Hu and X.-J. Liu, Phys. Rev. A **73**, 051603(R) (2006).

I. TWO-BODY BOUND STATE

Let us begin with the two-body problem, which helps to intuitively understand the many-body behavior of this system. The molecular state with center-of-mass (COM) momentum \mathbf{q} can be constructed as $|\Phi\rangle_{\mathbf{q}} = \frac{1}{2} \sum_{\mathbf{k}} \sum_{j,l=1}^2 \phi_{\mathbf{kq},jl} S_{\mathbf{kq},jl}^\dagger |0\rangle$ with

$$S_{\mathbf{kq},jl}^\dagger = \frac{1}{\sqrt{2}} [\psi_{j\uparrow}^\dagger(\mathbf{Q}_+) \psi_{l\downarrow}^\dagger(\mathbf{Q}_-) - \psi_{j\downarrow}^\dagger(\mathbf{Q}_+) \psi_{l\uparrow}^\dagger(\mathbf{Q}_-)], \quad (8)$$

where $\mathbf{Q}_\pm = \mathbf{q}/2 \pm \mathbf{k}$ and $S_{\mathbf{kq},jl}^\dagger$ is a singlet operator for creating a pair of atoms in the layers j and l with a COM momentum \mathbf{q} and a relative momentum \mathbf{k} , and $\phi_{\mathbf{kq},jl}$ is the corresponding probability amplitude. Here, we have used the fact that the four singlet operators introduced above form an invariant subspace of the total Hamiltonian \mathcal{H} and hence serve as a complete basis for the bound state. Notice that due to relations $S_{-\mathbf{kq},jl}^\dagger = S_{\mathbf{kq},lj}^\dagger$ and $\phi_{-\mathbf{kq},jl} = \phi_{\mathbf{kq},lj}$, we have added a factor 1/2 in the summations $\sum_{\mathbf{k}}$ to avoid a double counting of the terms comprising the state vector $|\Phi\rangle_{\mathbf{q}}$.

Substituting the wave-function $|\Phi\rangle_{\mathbf{q}}$ into the stationary Schrödinger equation $\mathcal{H}|\Phi\rangle_{\mathbf{q}} = E_{\mathbf{q}}|\Phi\rangle_{\mathbf{q}}$ one can get the following explicit form for each component:

$$\begin{aligned} E_{\mathbf{q}}\phi_{\mathbf{kq},11} &= \{\mathbf{k}^2 + (\mathbf{q}/2 + \kappa\mathbf{e}_x)^2 - h\}\phi_{\mathbf{kq},11} + \frac{\mathcal{J}}{2}(\phi_{\mathbf{kq},12} + \phi_{\mathbf{kq},21}) + \frac{U}{S} \sum_{\mathbf{k}'} \phi_{\mathbf{k}'\mathbf{q},11} \\ E_{\mathbf{q}}\phi_{\mathbf{kq},12} &= \{(\mathbf{k} + \kappa\mathbf{e}_x)^2 + \mathbf{q}^2/4\}\phi_{\mathbf{kq},12} + \frac{\mathcal{J}}{2}(\phi_{\mathbf{kq},11} + \phi_{\mathbf{kq},22}) \\ E_{\mathbf{q}}\phi_{\mathbf{kq},21} &= \{(\mathbf{k} - \kappa\mathbf{e}_x)^2 + \mathbf{q}^2/4\}\phi_{\mathbf{kq},21} + \frac{\mathcal{J}}{2}(\phi_{\mathbf{kq},11} + \phi_{\mathbf{kq},22}) \\ E_{\mathbf{q}}\phi_{\mathbf{kq},22} &= \{\mathbf{k}^2 + (\mathbf{q}/2 - \kappa\mathbf{e}_x)^2 + h\}\phi_{\mathbf{kq},22} + \frac{\mathcal{J}}{2}(\phi_{\mathbf{kq},12} + \phi_{\mathbf{kq},21}) + \frac{U}{S} \sum_{\mathbf{k}'} \phi_{\mathbf{k}'\mathbf{q},22}. \end{aligned}$$

where $E_{\mathbf{q}}$ is an eigenenergy. Then, we have

$$\begin{aligned} E_{\mathbf{q}}(\phi_{\mathbf{kq},11} + \phi_{\mathbf{kq},22}) &= (\mathbf{k}^2 + \mathbf{q}^2/4 + \kappa^2)(\phi_{\mathbf{kq},11} + \phi_{\mathbf{kq},22}) + (q_x\kappa - h)(\phi_{\mathbf{kq},11} - \phi_{\mathbf{kq},22}) \\ &\quad + \Omega(\phi_{\mathbf{kq},12} + \phi_{\mathbf{kq},21}) + \frac{U}{S} \sum_{\mathbf{k}'} (\phi_{\mathbf{k}'\mathbf{q},11} + \phi_{\mathbf{k}'\mathbf{q},22}) \\ E_{\mathbf{q}}(\phi_{\mathbf{kq},11} - \phi_{\mathbf{kq},22}) &= (\mathbf{k}^2 + \mathbf{q}^2/4 + \kappa^2)(\phi_{\mathbf{kq},11} - \phi_{\mathbf{kq},22}) + (q_x\kappa - h)(\phi_{\mathbf{kq},11} + \phi_{\mathbf{kq},22}) \\ &\quad + \frac{U}{S} \sum_{\mathbf{k}'} (\phi_{\mathbf{k}'\mathbf{q},11} - \phi_{\mathbf{k}'\mathbf{q},22}) \\ (\phi_{\mathbf{kq},12} + \phi_{\mathbf{kq},21}) &= \left\{ \frac{\mathcal{J}/2}{E_{\mathbf{q}} - (\mathbf{k} + \kappa\mathbf{e}_x)^2 - \mathbf{q}^2/4} + \frac{\mathcal{J}/2}{E_{\mathbf{q}} - (\mathbf{k} - \kappa\mathbf{e}_x)^2 - \mathbf{q}^2/4} \right\} (\phi_{\mathbf{kq},11} + \phi_{\mathbf{kq},22}). \end{aligned}$$

Solving the above equations, one finds

$$\begin{aligned} (\phi_{\mathbf{kq},11} + \phi_{\mathbf{kq},22}) &= \frac{\gamma_{\mathbf{k}} \frac{U}{S} \sum_{\mathbf{k}'} (\phi_{\mathbf{k}'\mathbf{q},11} + \phi_{\mathbf{k}'\mathbf{q},22}) + \beta_{\mathbf{k}} \frac{U}{S} \sum_{\mathbf{k}'} (\phi_{\mathbf{k}'\mathbf{q},11} - \phi_{\mathbf{k}'\mathbf{q},22})}{\alpha_{\mathbf{k}}\gamma_{\mathbf{k}} - \beta_{\mathbf{k}}^2} \\ (\phi_{\mathbf{kq},11} - \phi_{\mathbf{kq},22}) &= \frac{\alpha_{\mathbf{k}} \frac{U}{S} \sum_{\mathbf{k}'} (\phi_{\mathbf{k}'\mathbf{q},11} - \phi_{\mathbf{k}'\mathbf{q},22}) + \beta_{\mathbf{k}} \frac{U}{S} \sum_{\mathbf{k}'} (\phi_{\mathbf{k}'\mathbf{q},11} + \phi_{\mathbf{k}'\mathbf{q},22})}{\alpha_{\mathbf{k}}\gamma_{\mathbf{k}} - \beta_{\mathbf{k}}^2}, \end{aligned}$$

with

$$\begin{aligned} \alpha_{\mathbf{k}} &= E_{\mathbf{q}} - (\mathbf{k}^2 + \mathbf{q}^2/4 + \kappa^2). \\ \beta_{\mathbf{k}} &= q_x\kappa - h \\ \gamma_{\mathbf{k}} &= \alpha_{\mathbf{k}} - \left\{ \frac{\mathcal{J}^2/2}{E_{\mathbf{q}} - (\mathbf{k} + \kappa\mathbf{e}_x)^2 - \mathbf{q}^2/4} + \frac{\mathcal{J}^2/2}{E_{\mathbf{q}} - (\mathbf{k} - \kappa\mathbf{e}_x)^2 - \mathbf{q}^2/4} \right\} \end{aligned}$$

After some straightforward derivations, we arrive at the following self-consistent equation for the molecular energy $E_{\mathbf{q}}$:

$$\left(\frac{U}{S} \sum_{\mathbf{k}} \frac{\alpha_{\mathbf{k}}}{\alpha_{\mathbf{k}}\gamma_{\mathbf{k}} - \beta_{\mathbf{k}}^2} - 1 \right) \left(\frac{U}{S} \sum_{\mathbf{k}} \frac{\gamma_{\mathbf{k}}}{\alpha_{\mathbf{k}}\gamma_{\mathbf{k}} - \beta_{\mathbf{k}}^2} - 1 \right) - \left(\frac{U}{S} \sum_{\mathbf{k}} \frac{\beta_{\mathbf{k}}}{\alpha_{\mathbf{k}}\gamma_{\mathbf{k}} - \beta_{\mathbf{k}}^2} \right)^2 = 0. \quad (9)$$

Notice that, $\alpha_{\mathbf{k}}$, $\beta_{\mathbf{k}}$ and $\gamma_{\mathbf{k}}$ do not depend on the detuning δ between two components, i.e. the two-body spectrum obtained using Eq. (9) would not be altered by changing δ . On the other hand, the detuning shifts the single particle spectrum by $\pm\delta/2$ for different spin components.

Minimizing $E_{\mathbf{q}}$ with respect to the COM momentum \mathbf{q} , one can obtain the ground state energy of the molecular state. The corresponding coefficients $\phi_{\mathbf{kq},jl}$ (not normalized) are given by

$$\begin{aligned}\sum_{\mathbf{k}'}(\phi_{\mathbf{k}'\mathbf{q},11} - \phi_{\mathbf{k}'\mathbf{q},22}) &= \sum_{\mathbf{k}'}(\phi_{\mathbf{k}'\mathbf{q},11} + \phi_{\mathbf{k}'\mathbf{q},22})(\frac{U}{S}\sum_{\mathbf{k}}\frac{-\beta_{\mathbf{k}}}{\alpha_{\mathbf{k}}\gamma_{\mathbf{k}} - \beta_{\mathbf{k}}^2})/(\frac{U}{S}\sum_{\mathbf{k}}\frac{\alpha_{\mathbf{k}}}{\alpha_{\mathbf{k}}\gamma_{\mathbf{k}} - \beta_{\mathbf{k}}^2} - 1) \\ (\phi_{\mathbf{kq},11} + \phi_{\mathbf{kq},22}) &= \frac{\gamma_{\mathbf{k}}\frac{U}{S}\sum_{\mathbf{k}'}(\phi_{\mathbf{k}'\mathbf{q},11} + \phi_{\mathbf{k}'\mathbf{q},22}) + \beta_{\mathbf{k}}\frac{U}{S}\sum_{\mathbf{k}'}(\phi_{\mathbf{k}'\mathbf{q},11} - \phi_{\mathbf{k}'\mathbf{q},22})}{\alpha_{\mathbf{k}}\gamma_{\mathbf{k}} - \beta_{\mathbf{k}}^2} \\ (\phi_{\mathbf{kq},11} - \phi_{\mathbf{kq},22}) &= \frac{\alpha_{\mathbf{k}}\frac{U}{S}\sum_{\mathbf{k}'}(\phi_{\mathbf{k}'\mathbf{q},11} - \phi_{\mathbf{k}'\mathbf{q},22}) + \beta_{\mathbf{k}}\frac{U}{S}\sum_{\mathbf{k}'}(\phi_{\mathbf{k}'\mathbf{q},11} + \phi_{\mathbf{k}'\mathbf{q},22})}{\alpha_{\mathbf{k}}\gamma_{\mathbf{k}} - \beta_{\mathbf{k}}^2} \\ \phi_{\mathbf{kq},12} &= \frac{\mathcal{J}/2}{E_{\mathbf{q}} - (\mathbf{k} + \kappa\mathbf{e}_x)^2 - \mathbf{q}^2/4}(\phi_{\mathbf{kq},11} + \phi_{\mathbf{kq},22}) \\ \phi_{\mathbf{kq},21} &= \frac{\mathcal{J}/2}{E_{\mathbf{q}} - (\mathbf{k} - \kappa\mathbf{e}_x)^2 - \mathbf{q}^2/4}(\phi_{\mathbf{kq},11} + \phi_{\mathbf{kq},22}).\end{aligned}$$

For vanishing interlayer and intercomponent detunings, i.e. $h = \delta = 0$, one recovers the results in the main text. Some remarks for the case where $h = 0$: (i) For $\kappa = 0$, we have $\beta_{\mathbf{k}} = 0$ and Eq. (9) reduces to $\frac{U}{S}\sum_{\mathbf{k}}\frac{1}{\alpha_{\mathbf{k}}} - 1 = 0$ and $\frac{U}{S}\sum_{\mathbf{k}}\frac{1}{\gamma_{\mathbf{k}}} - 1 = 0$, with the binding energy $E_b^{(1)} = \sqrt{E_b^2 + \mathcal{J}^2} - \mathcal{J}$ and $E_b^{(2)} = E_b - \mathcal{J}$ modified simply by the tunneling strength \mathcal{J} . (ii) For $\mathcal{J} = 0$, the momentum transfer $2\kappa\mathbf{e}_x$ brought by the Raman coupling can be simply gauged away via a unitary transformation describing the layer-dependent momentum shift, and the binding energy is $E_b^{(1)} = E_b^{(2)} = E_b$. (iii) For $\kappa \neq 0$ and $\mathcal{J} \neq 0$, the inter-component attractive interaction would act together with the interlayer tunneling and intra-component spin-orbit coupling. This can give rise to nontrivial two-body and many-body ground states discussed in the main text.

II. BOGOLIUBOV-DE GENNES EQUATIONS OF THE SYSTEM

Since the atomic attraction takes place only in the same layer, we introduce the superfluid order parameters $\Delta_j(\mathbf{r}) = -U\langle\psi_{j,\downarrow}(\mathbf{r})\psi_{j,\uparrow}(\mathbf{r})\rangle$ ($j = 1, 2$) with $\mathbf{r} = (x, y)$. Then, the Hamiltonian (1) can be diagonalized via a Bogoliubov–Valatin transformation. By taking into account an additional weak harmonic trapping potential $V(r) = m\omega^2r^2/2$, the resultant Bogoliubov-de Gennes (BdG) equation can be written as: $H_{\text{BdG}}(\mathbf{r})\phi_{\eta} = \varepsilon_{\eta}\phi_{\eta}$. Here,

$$H_{\text{BdG}}(\mathbf{r}) = \begin{pmatrix} H_1(\mathbf{r}) & H_{\mathcal{J}} \\ H_{\mathcal{J}}^{\dagger} & H_2(\mathbf{r}) \end{pmatrix} \quad (10)$$

is an 8×8 matrix with $H_{\mathcal{J}} = \text{diag}(J/2, J/2, -J/2, -J/2)$ describing the interlayer tunneling, and $H_{1,2}(\mathbf{r})$ denoting the single-particle Hamiltonian for each layer $j = 1, 2$. The latter Hamiltonians read explicitly

$$H_j(\mathbf{r}) = \begin{pmatrix} \epsilon_{j\uparrow}(\mathbf{r}) & 0 & 0 & -\Delta_j(\mathbf{r}) \\ 0 & \epsilon_{j\downarrow}(\mathbf{r}) & \Delta_j(\mathbf{r}) & 0 \\ 0 & \Delta_j^*(\mathbf{r}) & -\epsilon_{j\uparrow}^*(\mathbf{r}) & 0 \\ -\Delta_j^*(\mathbf{r}) & 0 & 0 & -\epsilon_{j\downarrow}^*(\mathbf{r}) \end{pmatrix}, \quad (11)$$

with $j = 1, 2$ and

$$\begin{cases} \epsilon_{1\uparrow,\downarrow}(\mathbf{r}) = -\hbar^2\nabla^2/(2m) - i\hbar^2\kappa\partial_x/m + V(\mathbf{r}) - \mu \\ \epsilon_{2\uparrow,\downarrow}(\mathbf{r}) = -\hbar^2\nabla^2/(2m) + i\hbar^2\kappa\partial_x/m + V(\mathbf{r}) - \mu \end{cases}. \quad (12)$$

Here, we have taken $h = \delta = 0$. In this case, the ground state is spin balanced with equal chemical potential μ for both components. The Nambu basis is chosen as $\phi_{\eta} = [u_{1\uparrow,\eta}, u_{1\downarrow,\eta}, v_{1\uparrow,\eta}, v_{1\downarrow,\eta}, u_{2\uparrow,\eta}, u_{2\downarrow,\eta}, v_{2\uparrow,\eta}, v_{2\downarrow,\eta}]^T$, and ε_{η} is the corresponding energy of the Bogoliubov quasiparticles labeled by an index η . The order parameter $\Delta_{1,2}(\mathbf{r})$ is to be determined self-consistently by

$$\Delta_j(\mathbf{r}) = -U\sum_{\eta}[u_{j\uparrow,\eta}v_{j\downarrow,\eta}^*f(-\varepsilon_{\eta}) + u_{j\downarrow,\eta}v_{j\uparrow,\eta}^*f(\varepsilon_{\eta})],$$

where $f(E) = 1/[e^{E/k_B T} + 1]$ is the Fermi-Dirac distribution function at a temperature T . The chemical potential μ is obtained using the number equation $N = \int d\mathbf{r} n(\mathbf{r})$, where the total atomic density is given by

$$n(\mathbf{r}) = \sum_{j\gamma,\eta} [|u_{j\gamma,\eta}(\mathbf{r})|^2 f(\varepsilon_\eta) + |v_{j\gamma,\eta}(\mathbf{r})|^2 f(-\varepsilon_\eta)]. \quad (13)$$

The ground state can then be found by solving the above BdG equation self-consistently with the basis expansion method [42]. In the numerical simulations, we have taken a large energy cutoff $\varepsilon_c = 6E_{\text{rec}}$ to ensure the accuracy of the calculation, where $E_{\text{rec}} = 5\hbar\omega$ assures that the trap oscillation frequency ω is much smaller than the recoil frequency.
